Segregation in bimetallic nanowires: Size and thermodynamic ensemble effects

Emile Maras,[1,*] Fabienne Berthier,[1,2] Isabelle Braems,[1,2] and Bernard Legrand[3]
[1]*LEMHE/ICMMO, Univ. Paris Sud, UMR 8182, F91405 Orsay Cedex, France*
[2]*CNRS, UMR 8182, F91405 Orsay Cedex, France*
[3]*CEA, DEN, Service de Recherches de Métallurgie Physique, F91191 Gif-sur-Yvette Cedex, France*
(Received 29 May 2012; revised manuscript received 1 August 2012; published 29 August 2012)

We investigate the thermodynamics of bimetallic nanowires via a rigid lattice approach. This allows us to detail the behavior of edge and core sites of the chain in the case of an alloy that forms an ideal solution. The influence of chain length on segregation (i.e., the composition difference between core and edge sites) is analyzed in the semigrand canonical (sGC) and in the canonical ensembles. Segregation varies monotonically with chain length in both ensembles, being enhanced at low concentrations and diminishing at large ones. For intermediate concentrations, segregation increases with chain length in the sGC ensemble, whereas it decreases in the canonical ensemble. This illustrates that the concentration profiles differ in both ensembles, the effect being emphasized at smaller sizes.

DOI: 10.1103/PhysRevB.86.054205 PACS number(s): 68.35.bd, 68.35.Dv

I. INTRODUCTION

Binary nanoparticles and nanowires are the subject of much attention.[1–6] Recent advances in the synthesis and characterization of size-selected particles in the nanometer range make it now possible to investigate their physical and chemical properties. Such particles are characterized by a large number of surface atoms with regard to the number of bulk (or core) atoms. It is then obvious that the effects of the surface on the cohesive properties of the particle cannot be neglected. This is observed in various situations, such as the well-known size-dependent melting point depression[7] and alloy phase transitions of nanoparticles.[8] Because nanoparticles are intermediate between bulk and surface, the phase diagram might vary with their size.

Theoretical studies using a rigid lattice approach and a simple energetic model are common useful tools to explore the basic features of the bulk[9] and surface[10] phase diagrams of alloys. These models are indeed particularly adapted to study the thermodynamics of finite binary systems and to determine how the size and segregation effects modify the phase diagrams.[1,11–14] They rely on the definition of a total free energy functional where all segregation-related quantities (chemical interactions, surface heterogeneities) are incorporated within the mixing enthalpy, the entropic part often simply described by a mixing entropy.[12] For infinite systems, the equilibrium state of the binary system is then obtained by minimizing this free energy, no matter what thermodynamic ensemble is chosen, since Van Hove's theorem guarantees that the different statistical ensembles converge toward the same equilibrium state when the thermodynamic limit applies.[15]

For finite systems, the different ensembles are not equivalent. A study based on lattice gas models has shown that it is possible to define phase transitions rigorously, even in finite systems, with the prediction of intriguing phenomena such as bimodalities and negative heat capacities according to the statistical ensemble to be considered.[16,17] This also affects the behavior of the thermodynamic variables that quantify the segregation. Recent atomistic studies have predicted, for instance, interesting differences in the behavior of three-dimensional clusters between canonical and semigrand canonical (sGC) ensembles, in the case of alloys, with a tendency to phase separate.[18–21] Since the fine experimental quantification of the composition profiles of binary nanoparticles is still a challenging task, care must be taken in theoretical studies when choosing the thermodynamic ensemble that will accurately represent the experimental situation.

The aim of the present work is to investigate the evolution of superficial segregation with cluster size and quantify the differences in behavior when one switches from canonical to sGC ensembles.

It is well beyond the scope of this paper to account for all the parameters that may be involved in the segregation process: elastic, alloy, and surface effects are indeed strongly coupled to the surface structure of the system.[22] To isolate the origin of the difference of composition profiles with regard to the ensemble under investigation, we consider finite linear chains using a rigid lattice approach, for which the exact free energy can be derived while considering surface effects. An upsurge in studies based on this one-dimensional (1D) model in the current literature[23–27] has occurred because it provides an exact quantification of domain walls in magnetism and 1D Ising-like antiferromagnets, in which long-range order is neglected.[25] Taking into account segregation within the wire will allow the interpretation of experiments on bimetallic atomic wires that can decorate the steps of a surface.[27,28] Correspondingly we shall consider the canonical ensemble in which the nominal concentration (i.e., the proportion of the different atoms) is fixed, whereas in the sGC ensemble, the nominal concentration is controlled by the value of the difference of the chemical potentials between the two species. We elucidate why the different ensembles are not equivalent for small chains by relating it to the mixing entropy at the expense of chemical interactions. We analyze the difference of the equilibrium concentration profiles observed, even in the case of an alloy forming an ideal solid solution, where only surface effects are responsible for segregation, and we provide guidelines to extend these results to particles of higher dimensions.

The paper is organized as follows. The theoretical approach and specificities of each ensemble are detailed in

section II. In section III, we compare canonical and sGC isotherms and develop a Taylor series expansion of the canonical variables, called the Delta method, to analyze in detail the differences between both ensembles. The size and temperature effects on the equilibrium concentration profiles and on the nonequivalency of the ensembles are presented in section IV.

II. ENERGETIC AND STATISTICAL MODELS

A. Energetic model

We consider a linear chain of length n which contains n_{A} A atoms and n_{B} B atoms, with $n = n_{\mathrm{A}} + n_{\mathrm{B}}$ and whose nominal concentration is $c = n_{\mathrm{A}}/n$. The $\mathrm{A}_c\mathrm{B}_{1-c}$ system is described via an Ising Hamiltonian,[9]

$$H(n) = \frac{1}{2}\sum_{I,J}\sum_{i,j\neq i}^{n} p_i^I\, p_j^J\, V_{ij}^{IJ}, \tag{1}$$

where V_{ij}^{IJ} is the interaction energy between an atom of type I at a site i and an atom of type J at a site j $[(I,J) = (\mathrm{A},\mathrm{B})]$, i and j being in the nearest neighbor position. p_i^I is the occupation number that equals 1 (0) if the i site is (not) occupied by an atom of type I. For a binary alloy, $p_i^{\mathrm{A}} = 1 - p_i^{\mathrm{B}}$ and we set $p_i^{\mathrm{A}} = p_i$, which leads to

$$H(n) = H_0 + V\sum_{i=1}^{n}\sum_{j\neq i} p_i\, p_j + (\tau - V)\sum_{i=1}^{n} z_i\, p_i, \tag{2}$$

with $H_0 = (n-1)V^{\mathrm{BB}}$, $V = (V^{\mathrm{AA}} + V^{\mathrm{BB}} - 2V^{\mathrm{AB}})/2$, $\tau = (V^{\mathrm{AA}} - V^{\mathrm{BB}})/2$, and z_i is the coordination number of the ith site, equal to 1 (2) for an edge (core) site. H_0 is a constant, V is the energy of the alloy pair interaction, and τ is proportional to the difference between cohesive energies of pure metals. As we consider an alloy that forms an ideal solution, $V = 0$, the Hamiltonian can be written (considering H_0 as the reference for the energy)

$$H(n) = \tau(p_1 + p_n) + 2\tau\sum_{i=2}^{n-1} p_i. \tag{3}$$

This relation emphasizes the edge ($i = 1$ and n) and core ($i = 2, \ldots, n-1$) sites. Note that $n_{\mathrm{A}} = \sum_{i=1}^{n} p_i$; therefore, we can rewrite H as

$$H(n,n_{\mathrm{A}},n_{\mathrm{A},e}) = 2\left(n_{\mathrm{A}} - \frac{n_{\mathrm{A},e}}{2}\right)\tau, \tag{4}$$

with the number $n_{\mathrm{A},e}$ of A atoms on the edge sites that equals 0, 1, or 2. The number of A atoms on the core sites is then $n_{\mathrm{A},c} = n_{\mathrm{A}} - n_{\mathrm{A},e}$.

We denote $c_i = \langle p_i\rangle$ the concentration of the ith site starting from the left of the chain, $c_e = \langle n_{\mathrm{A},e}\rangle/2$ the concentration of the edge sites, and $c_c = \langle n_{\mathrm{A},c}\rangle/(n-2)$ the concentration of the core sites. The edge and core concentrations are related to the nominal concentration of the chain by the mass conservation law :

$$nc = 2c_e + (n-2)\,c_c. \tag{5}$$

Whatever the ensemble considered, an exact formula of the equilibrium concentration profile requires the determination of the partition function Z^{E}, in which E represents either the canonical or the sGC ensemble, and of $Z^{\mathrm{E}}_{p_i=1}$, in which the restricted partition function for each site i corresponds to configurations in which site i is occupied by an A atom ($p_i = 1$):[9,29]

$$c_i^{\mathrm{E}} = Z^{\mathrm{E}}_{p_i=1}/Z^{\mathrm{E}}. \tag{6}$$

B. Semigrand canonical ensemble

In the sGC ensemble, the n-chain is in equilibrium with a reservoir. The composition of the chain is controlled by the chemical potential difference between A and B: $\Delta\mu = \mu_{\mathrm{A}} - \mu_{\mathrm{B}}$. The free energy in the sGC ensemble is given by:

$$F(n,\Delta\mu) = H(n) - \Delta\mu\sum_{i=1}^{n} p_i. \tag{7}$$

Because $V = 0$, the two edge sites and the $n-2$ core sites are not correlated, and the partition function is the product of partition functions for each site. From Eqs. (3) and (7),[23]

$$Z^{\mathrm{sGC}}(n,\underline{\Delta\mu}) = (1 + e^{-\underline{\tau}+\underline{\Delta\mu}})^2(1 + e^{-2\underline{\tau}+\underline{\Delta\mu}})^{n-2}, \tag{8}$$

with $\underline{x} = x/k_{\mathrm{B}}T$ and $x = \tau, \Delta\mu$. The restricted partition function $Z^{\mathrm{sGC}}_{p_i=1}(n,\underline{\Delta\mu})$ takes two different values, one for the edge sites ($Z_e^{\mathrm{sGC}}(n,\underline{\Delta\mu})$ for $i = 1$ or n) and one for the core sites ($Z_c^{\mathrm{sGC}}(n,\underline{\Delta\mu})$ for $i = 2, \ldots, n-1$):

$$\begin{aligned} Z_e^{\mathrm{sGC}}(n,\underline{\Delta\mu}) &= \frac{e^{-\underline{\tau}+\underline{\Delta\mu}}}{1 + e^{-\underline{\tau}+\underline{\Delta\mu}}} Z^{\mathrm{sGC}}(n,\underline{\Delta\mu}),\\ Z_c^{\mathrm{sGC}}(n,\underline{\Delta\mu}) &= \frac{e^{-2\underline{\tau}+\underline{\Delta\mu}}}{1 + e^{-2\underline{\tau}+\underline{\Delta\mu}}} Z^{\mathrm{sGC}}(n,\underline{\Delta\mu}). \end{aligned} \tag{9}$$

Equations (6)–(9) provide the concentration profile as a function of $\underline{\Delta\mu}$:

$$\begin{aligned} c_e^{\mathrm{sGC}}(n,\underline{\Delta\mu}) &= \frac{1}{1 + e^{\underline{\tau}-\underline{\Delta\mu}}},\\ c_c^{\mathrm{sGC}}(n,\underline{\Delta\mu}) &= \frac{1}{1 + e^{2\underline{\tau}-\underline{\Delta\mu}}}. \end{aligned} \tag{10}$$

Whereas for a given value of $\underline{\Delta\mu}$ the edge and core concentrations depend only on $\underline{\tau}$ [Eq. (10)], the nominal concentration c^{sGC} given by the mass conservation law [Eq. (5)] depends also on the length of chain n. Analytical formulae of the edge and core concentrations as functions of the nominal concentration are given in Appendix A. These relations show that at a fixed value of the nominal concentration, the concentration profile depends on the chain length.

C. Canonical ensemble

Because the Hamiltonian of the bimetallic finite n-chain [Eq. (4)] depends on the number of A atoms on the edge sites, the partition function for an n-chain containing n_{A} A atoms can be written

$$Z^{\mathrm{Cano}}(n,n_{\mathrm{A}}) = \sum_{n_{\mathrm{A},e}=0}^{2} Z^{\mathrm{Cano}}_{n_{\mathrm{A},e}}(n,n_{\mathrm{A}}), \tag{11}$$

where $Z^{\text{Cano}}_{n_{A,e}}(n,n_A)$ is the restricted partition function of configurations containing $n_{A,e}$ A atoms on edge sites, and the restricted partition function $Z^{\text{Cano}}_{p_i=1}(n,n_A)$ is the sum of the more constrained partition function, $Z^{\text{Cano}}_{p_i=1,n_{A,e}}(n,n_A)$, of configurations with an A atom on site i and $n_{A,e}$ A atoms on edge sites:

$$Z^{\text{Cano}}_{p_i=1}(n,n_A) = \sum_{n_{A,e}=0}^{2} Z^{\text{Cano}}_{p_i=1,n_{A,e}}(n,n_A). \tag{12}$$

$Z^{\text{Cano}}_{n_{A,e}}(n,n_A)$ and $Z^{\text{Cano}}_{p_i=1,n_{A,e}}(n,n_A)$ are detailed in Appendix B. Using Eqs. (5) and (6), we can relate the edge and core concentrations to n, c, and $\underline{\tau}$ with $c = n_A/n$, where n_A is an integer:

$$c_e^{\text{Cano}}(n,c) = ce^{\underline{\tau}}\frac{n\left(ce^{\underline{\tau}}+1-c\right)-e^{\underline{\tau}}}{n\left(ce^{\underline{\tau}}+1-c\right)^2-\left(ce^{2\underline{\tau}}+1-c\right)},$$
$$c_c^{\text{Cano}}(n,c) = \frac{c}{n-2}\left[n-2e^{\underline{\tau}}\frac{n\left(ce^{\underline{\tau}}+1-c\right)-e^{\underline{\tau}}}{n\left(ce^{\underline{\tau}}+1-c\right)^2-\left(ce^{2\underline{\tau}}+1-c\right)}\right]. \tag{13}$$

Equation (13) verifies the mass conservation law.

In the sGC ensemble, the most natural representation is to depict the concentrations of the different sites as a function of $\underline{\Delta\mu}$. However, experimental results are usually obtained by controlling the nominal concentration. Because the nominal concentration in the sGC ensemble is deduced from the equilibrium profile using the mass conservation law, it is possible to compare the edge and core concentrations for both ensembles according to the nominal concentration. Conversely, comparing isotherms from both ensembles according to the chemical potential difference requires the computation of $\underline{\Delta\mu}$ when the nominal concentration is fixed (i.e., in the canonical ensemble). $\underline{\Delta\mu}$ is the derivative of the normalized free energy as a function of the nominal concentration, $\underline{\Delta\mu}^{\text{Cano}} = \frac{1}{n}\frac{\partial \underline{F}^{\text{Cano}}}{\partial c}$, with $\underline{F}^{\text{Cano}} = -\ln Z^{\text{Cano}}$. Recall that in the canonical ensemble the nominal concentration c only takes discrete values, so to calculate the chemical potential, we have to use a discrete derivative :

$$\underline{\Delta\mu}^{\text{Cano}}(n,n_A) = [\underline{F}^{\text{Cano}}(n,n_A+1) - \underline{F}^{\text{Cano}}(n,n_A-1)]/2. \tag{14}$$

The application of this formula to the system leads to the following expression:

$$\underline{\Delta\mu}^{\text{Cano}}(n,n_A) = 2\underline{\tau} + \frac{1}{2}\ln\left[\frac{n_A(n_A+1)}{n_B(n_B+1)}\right] + \frac{1}{2}\ln\left\{\frac{n_B(n_B+1)+e^{\underline{\tau}}(n_A-1)\left[2(n_B+1)+(n_A-2)e^{\underline{\tau}}\right]}{(n_B-1)(n_B-2)+e^{\underline{\tau}}(n_A+1)[2(n_B-1)+n_Ae^{\underline{\tau}}]}\right\}. \tag{15}$$

III. CANONICAL AND SEMIGRAND CANONICAL ISOTHERMS

Broken bonds at the chain edges yield a segregation phenomenon (i.e., an enrichment in one of the two species on the edge sites with regard to the core sites). Within this study we consider positive values of $\underline{\tau} > 0$, which leads to the segregation of the A species of lowest cohesive energy, whatever the bulk concentration. Here, we determine whether the chemical repartition of A and B atoms is identical in both statistical ensembles when the value of either $\underline{\Delta\mu}$ or c is set. We compare the isotherm $c(\underline{\Delta\mu})$ and the edge and core isotherms as a function of the difference of chemical potentials, $c_p(\underline{\Delta\mu})$, and of the nominal concentration, $c_p(c)$, in both ensembles.

Figure 1(a) shows that even for an alloy forming an ideal solution, a small difference exists between isotherms $c(\underline{\Delta\mu})$ of both ensembles for a 10-atom wire. The canonical isotherm is steeper than the sGC isotherm. Edge site and core site isotherms are also steeper in the canonical ensemble than in the sGC ensemble [Fig. 1(b)], which means that $|c_p^{\text{Cano}} - 0.5| > |c_p^{\text{sGC}} - 0.5|$. Expressed as a function of the nominal concentration, the core and edge isotherms also differ in both ensembles, the edge concentration being systematically greater and the core concentration lower in the canonical ensemble relative to the sGC ensemble [Fig. 1(c)].

Figure 2(a) shows that for low [respectively (resp.) high] values of $\underline{\Delta\mu}$, the nominal concentration is lower (resp. higher) in the canonical ensemble than in the sGC ensemble. The $\underline{\Delta\mu}$ value for which the concentrations in both ensembles are equal corresponds to a nominal concentration close to 0.5. The deviation between the edge and core concentrations, $c_e - c_c$, that quantifies the segregation, is larger in the canonical ensemble than in the sGC ensemble [Fig. 2(b)].

$c_e - c_c$ displays a maximum in both ensembles. At low nominal concentration, edge site concentrations increase with c faster than the core site concentrations because of the broken bonds. When there are enough A atoms to almost fill both edge sites, at $c \approx 0.2$ for $n = 10$, the increase of c essentially contributes to increasing the core concentration, and thus $c_e - c_c$ decreases.

To prepare for the forthcoming discussion on the influence of the thermodynamic ensemble on segregation for a finite chain, we first recall that in the sGC ensemble, the number of atoms of each species (which is driven by the difference in chemical potentials of the constituents) fluctuates around a mean value. An efficient way to highlight these fluctuations is to consider the configurational density of states (CDOS) $n(c)$ for each nominal concentration c.[30] Thus $n(c)\,dc$ is the number of states for which the concentration is between c and $c + dc$. CDOS is determined from the sGC partition function given by Eq. (8) or, equivalently, by

$$Z^{\text{sGC}}(n,\underline{\Delta\mu}) = \sum_{n_A=0}^{n} Z^{\text{sGC}}(n,\underline{\Delta\mu},n_A), \tag{16}$$

where $Z^{\text{sGC}}(n,\underline{\Delta\mu},n_A)$ is the partition function of the system constrained by the composition, which can be written accord-

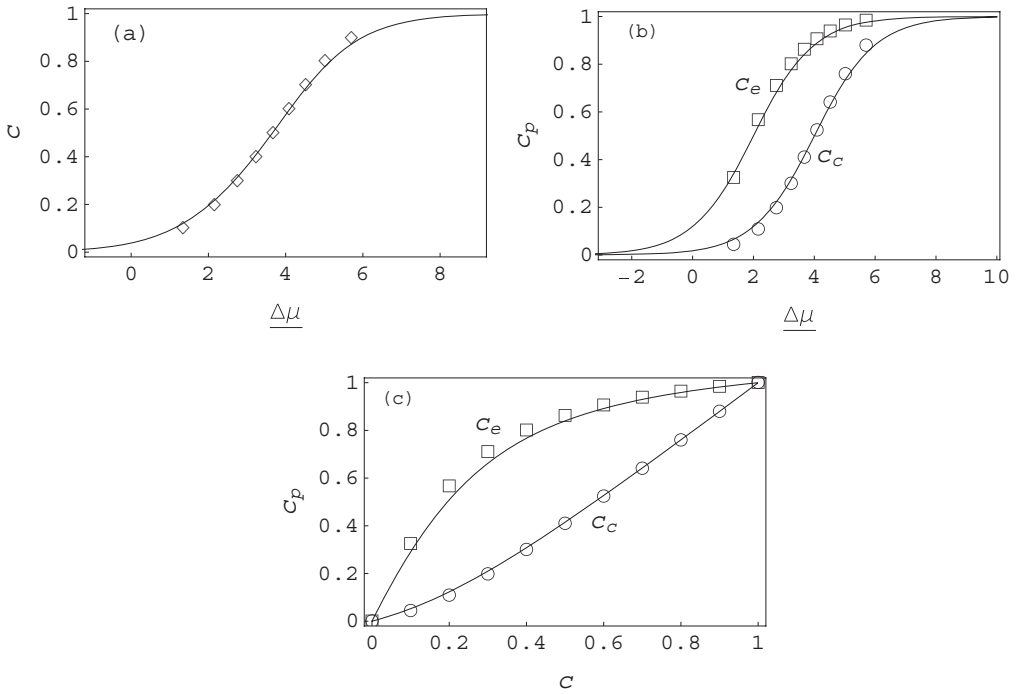

FIG. 1. (a) Evolution of the nominal concentration as a function of the chemical potential difference $\underline{\Delta\mu}$. Edge and core isotherms as a function of (b) the chemical potential difference $\underline{\Delta\mu}$ and (c) the nominal concentration. Lines, sGC isotherms; symbols, canonical isotherms [(a) nominal concentration, diamond; (b, c) edge concentration, square; (b, c) core concentration, circle]. The length of the chain is $n = 10$, $\underline{\tau} = 2$.

ing to the corresponding canonical partition function:

$$Z^{\mathrm{sGC}}(n,\underline{\Delta\mu},n_{\mathrm{A}}) = e^{n_{\mathrm{A}}\underline{\Delta\mu}} Z^{\mathrm{Cano}}(n,n_{\mathrm{A}}). \tag{17}$$

These relationships show that the sGC ensemble, for a given value of $\underline{\Delta\mu}$, is a weighted combination of canonical subensembles of different compositions. The total number of configurations in the sGC ensemble is then much larger than the one derived in the canonical ensemble. The composition distribution $P^{\mathrm{sGC}}_{n_{\mathrm{A}}}(n,\underline{\Delta\mu})$ gives the probability that the n-chain contains n_A atoms for a given $\underline{\Delta\mu}$:

$$P^{\mathrm{sGC}}_{n_{\mathrm{A}}}(n,\underline{\Delta\mu}) = \frac{Z^{\mathrm{sGC}}(n,\underline{\Delta\mu},n_{\mathrm{A}})}{Z^{\mathrm{sGC}}(n,\underline{\Delta\mu})}. \tag{18}$$

The nominal concentration distribution for a 10-atom chain, when $c^{\mathrm{sGC}} = 0.5$ (or $\underline{\Delta\mu} \approx 3.7$), is presented in Fig. 3. The sGC nominal concentration c^{sGC} is the weighted average of the nominal concentrations of all possible subensembles.

The sGC concentration profile is therefore related to the concentration profile of the canonical ensemble via the nominal composition distribution

$$c_p^{\mathrm{sGC}}(n,\underline{\Delta\mu}) = \sum_{n_{\mathrm{A}}=0}^{n} P^{\mathrm{sGC}}_{n_{\mathrm{A}}}(n,\underline{\Delta\mu}) \times c_p^{\mathrm{Cano}}(n,n_{\mathrm{A}}). \tag{19}$$

For a 1D system, the sGC partition function and the nominal concentration distribution are easily and exactly determined; however, it is not as tractable for higher dimensions.[31] Therefore, it is useful to develop an approximated method that may be generalized to the 2D and 3D cases.

First, recall that a distribution as seen in Fig. 3 can be approximated by a Gaussian distribution.[14,15,20,21] The very

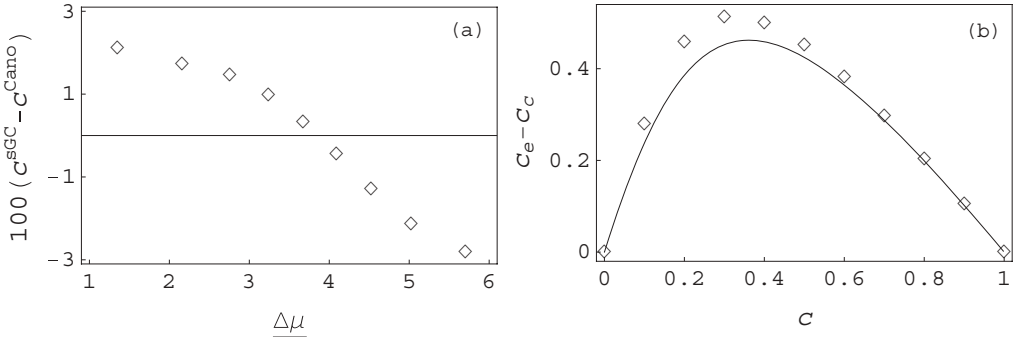

FIG. 2. Evolution in both ensembles of (a) the difference between the nominal concentration in canonical and sGC ensembles, $c^{\mathrm{sGC}} - c^{\mathrm{Cano}}$, as a function of the chemical potential difference $\underline{\Delta\mu}$ and (b) of $c_e - c_c$ as a function of the nominal concentration. Line, sGC ensemble; diamond, canonical ensemble. $n = 10$ and $\underline{\tau} = 2$.

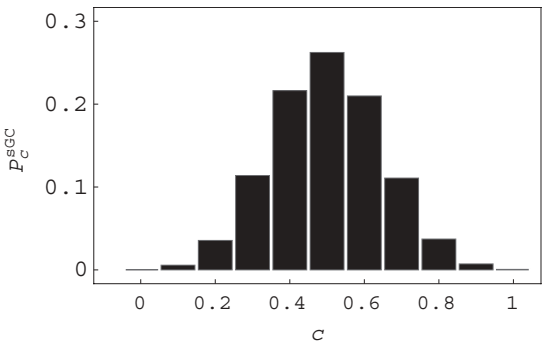

FIG. 3. Configurational densities of states for the sGC ensemble. $c^{sGC} = 0.5$, $n = 10$, and $\underline{\tau} = 2$.

general validity of the Gaussian approximation is due to the Laplace limit theorem.[32,33] Thus, at a given $\underline{\Delta\mu}$, the main features of a Gaussian distribution are the mean nominal concentration $\langle c\rangle = c^{sGC}$ and the variance defined by $\sigma^2 = \sum_c P_c^{sGC}(c - \langle c\rangle)^2$. σ^2can also be estimated from the isotherm using $\sigma^2 = \frac{1}{n}\frac{\partial c}{\partial \underline{\Delta\mu}}$.

In 1D, the analytical expression of σ^2 is

$$\sigma^2 = \frac{1}{n^2}\left[\frac{2e^{\underline{\tau}-\underline{\Delta\mu}}}{(1+e^{\underline{\tau}-\underline{\Delta\mu}})^2} + \frac{(n-2)e^{2\underline{\tau}-\underline{\Delta\mu}}}{(1+e^{2\underline{\tau}-\underline{\Delta\mu}})^2}\right]. \quad (20)$$

At the thermodynamic limit ($n \to \infty$), $\sigma^2 \to 0$; thus, the distribution tends to a δ-function, implying that the properties of the system are univocally defined by the value of $\underline{\Delta\mu}$. In other words, it means that canonical and sGC ensembles become equivalent.

To approximate sGC isotherms from canonical isotherms, we apply the Delta method.[34] For any variable in the sGC ensemble $f^{sGC}(\underline{\Delta\mu}) = f^{sGC}(\langle c\rangle)$, the Delta method consists in using a second-order Taylor series expansion of the canonical variable $f^{Cano}(c)$, centered in the mean value $\langle c\rangle$. $f^{sGC}(\langle c\rangle)$ is then given by

$$f^{sGC}(\langle c\rangle) \approx f^{Cano}(\langle c\rangle) + \frac{\sigma^2}{2}\left.\frac{\partial^2 f^{Cano}(c)}{\partial c^2}\right|_{\langle c\rangle}. \quad (21)$$

This relation underlines that for any variable, the difference between the sGC and the canonical ensembles is related to

(1) the fluctuations of the nominal concentration is the sGC ensemble—the higher the variance, the higher the difference, and

(2) the curvature of the canonical variable at the mean value $\langle c\rangle$—the difference between both ensembles increases with this curvature.

We apply Eq. (21) to analyze the deviation between the sGC and canonical profiles. Let us detail the two contributions with the help of Fig. 4 for the edge and core sites. Figure 4(a) shows the evolution of the variance versus the nominal concentration. The curve displays a maximum for a nominal concentration slightly greater than 0.5. The curvature of the canonical isotherms $\partial^2 c_p^{Cano}/\partial c^2$ is negative for the edge sites due to the segregation effect [Fig. 4(b)] and positive for the core sites [Fig. 4(c)]. The variance being positive by definition, the sign of the curvature gives the sign of the difference between both ensembles. Because of the smoothness of the curve $\sigma^2(c)$, the difference between both ensembles is driven by $\partial^2 c_p^{Cano}/\partial c^2$. The maximum of the deviation is around 0.06 for edge sites and 0.015 for core sites. The nominal concentration corresponding to this maximum is $c \approx 2/n$. Finally, we can see in Figs. 4(d) and 4(e) that the approximate and exact deviations between the canonical and sGC profiles are in good agreement.

So, the Delta method provides an effective link between the canonical and sGC ensembles, allowing one to analyze the differences between both.

IV. SIZE AND TEMPERATURE EFFECTS

A. Influence of the chain length

We analyze the influence of the chain length on the isotherms via a first-order expansion in $1/n$ of the exact Eqs. (10) and (13). In the canonical ensemble, the edge and core concentrations are written

$$\begin{aligned} c_e^{Cano} &= \frac{ce^{\underline{\tau}}}{1-c+ce^{\underline{\tau}}}\left(1 - \frac{1-c}{n}\frac{e^{\underline{\tau}}-1}{(1-c+ce^{\underline{\tau}})^2}\right), \\ c_c^{Cano} &= c\left(1 - 2\frac{1-c}{n}\frac{e^{\underline{\tau}}-1}{1-c+ce^{\underline{\tau}}}\right), \end{aligned} \quad (22)$$

whereas their counterparts in the sGC are

$$\begin{aligned} c_e^{sGC} &= \frac{ce^{\underline{\tau}}}{1-c+ce^{\underline{\tau}}}\left(1 - 2\frac{1-c}{n}\frac{e^{\underline{\tau}}-1}{(1-c+ce^{\underline{\tau}})^2}\right), \\ c_c^{sGC} &= c\left(1 - 2\frac{1-c}{n}\frac{e^{\underline{\tau}}-1}{1-c+ce^{\underline{\tau}}}\right). \end{aligned} \quad (23)$$

These relations underline two features of the isotherms:

(1) In both ensembles, the asymptotic behaviors when $n \to \infty$ read $c_e^E \to ce^{\underline{\tau}}/(1-c+ce^{\underline{\tau}})$ and $c_c^E \to c$, which corresponds to the classical isotherms in mean field approximation of a long chain for an alloy forming an ideal solid solution.

(2) When $\underline{\tau} > 0$, $e^{\underline{\tau}} - 1 > 0$. Thus, for a fixed value of the nominal concentration, c_e^E and c_c^E increase with chain length in both ensembles. Recall that the edge and core concentrations are related via the mass conservation law. Thus, at a given nominal concentration, the increase in chain length diminishes (increases) the proportion of the edge (core) sites, so that the nominal concentration is held constant while both edge and core concentrations increase.

Figure 5, which displays the behavior of the equilibrium profile as a function of the length of the chain for two concentrations, illustrates the above-mentioned features. Although not shown, the first-order expansion is in satisfying agreement with the exact results.

We showed previously that $c_e^E - c_c^E$ is a meaningful quantity to evaluate the segregation. Using the formulae above, the first-order expansion in $1/n$ can be written as

$$c_e^E - c_c^E = c(1-c)\frac{(e^{\underline{\tau}}-1)}{1-c+ce^{\underline{\tau}}}\left[1 + \frac{1}{n} \times \frac{\Delta^E}{(1-c+ce^{\underline{\tau}})^2}\right], \quad (24)$$

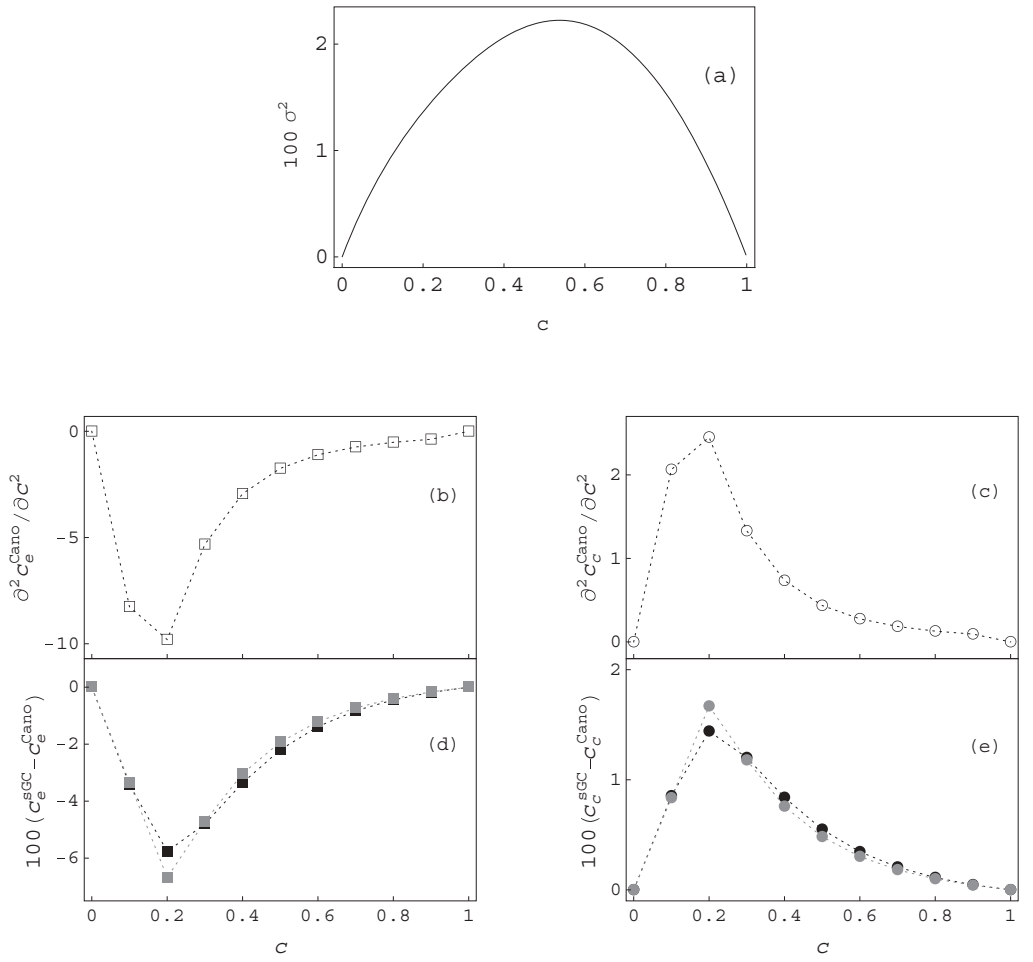

FIG. 4. Evolution with nominal concentration of (a) variance of the nominal concentration in the sGC ensemble, (b, c) the canonical isotherm curvature, and (d, e) the exact and approached difference between the sGC concentration and the canonical for the edge (b, d) and core (c, e) sites. Edge sites, squares (b, d); core sites, circles (c, e). Exact calculation given by Eq. (10) and (13) (solid black symbols) and approached calculations given by Eq. (21) (solid gray symbols) (d, e). Dotted lines are a visual help. $n = 10$ and $\underline{\tau} = 2$.

with

$$\Delta^{\text{Cano}} = 2\,(1 - c + ce^{\underline{\tau}})^2 - e^{\underline{\tau}},$$
$$\Delta^{\text{sGC}} = 2\,(1 - c + ce^{\underline{\tau}})^2 - 2e^{\underline{\tau}}. \tag{25}$$

So, when $n \to \infty$, $c_e^{\text{E}} - c_c^{\text{E}} \to (e^{\underline{\tau}} - 1)\frac{c(1-c)}{1-c+ce^{\underline{\tau}}}$ in both ensembles.

Figure 6(a) shows $c_e^{\text{E}} - c_c^{\text{E}}$ as a function of n for $c = 0.75$ with $\underline{\tau} = 2$. In both ensembles, the difference between the edge site and core site concentrations decreases when the length of the chain increases. At a given value of c, $c_e^{\text{E}} - c_c^{\text{E}}$ is a monotonic function of n, strictly decreasing (resp. increasing) when $\Delta^{\text{E}} > 0$ (resp. $\Delta^{\text{E}} < 0$). Segregation

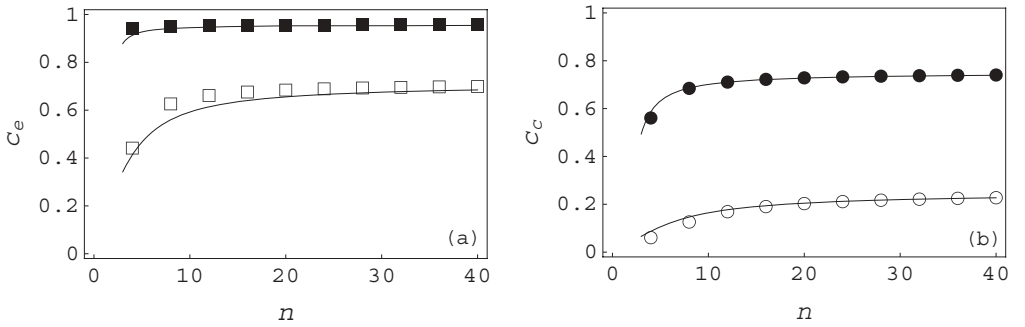

FIG. 5. Evolution of the exact edge (a) and core (b) concentrations in both ensembles as a function of the length of the chain for $c = 0.25$ and $c = 0.75$ ($\underline{\tau} = 2$). Line, sGC ensemble; symbols, canonical ensemble (squares, edge sites; circles, core sites). $c = 0.25$, empty symbols; $c = 0.75$, filled symbols.

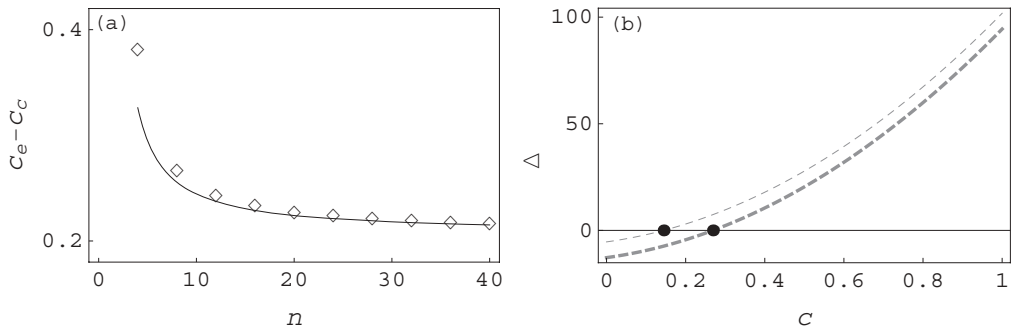

FIG. 6. (a) Evolution of $c_e - c_c$ with chain length in both ensembles at $c = 0.75$ (sGC, line; canonical, diamond). (b) Evolution of Δ^{E} as a function of the nominal concentration (Eq. (25)) in the sGC (thick dashed line) and canonical (thin dashed line) ensembles. $\underline{\tau} = 2$.

evolves with the length of the chain similarly in both ensembles when Δ^{Cano} and Δ^{sGC} are either positive or negative, which occurs for $c \geqslant 0.27$ and $c \leqslant 0.15$, as shown in Fig. 6(b). For $0.15 \leqslant c \leqslant 0.27$, $\Delta^{\mathrm{Cano}} > 0$ and $\Delta^{\mathrm{sGC}} < 0$, so $c_e^{\mathrm{Cano}} - c_c^{\mathrm{Cano}}$ diminishes, whereas $c_e^{\mathrm{sGC}} - c_c^{\mathrm{sGC}}$ increases with chain length.

For a better understanding of the difference in behaviors in both ensembles and to have a link with the Delta method, we use the following formulae, which are deduced from Eqs. (22)–(25) using a first-order expansion in $1/n$:

$$\begin{aligned} c_e^{\mathrm{sGC}} - c_e^{\mathrm{Cano}} &= -\frac{c\,(1-c)}{n}\frac{e^{\underline{\tau}}\,(e^{\underline{\tau}}-1)}{(1-c+ce^{\underline{\tau}})^3}, \\ c_c^{\mathrm{sGC}} &= c_c^{\mathrm{Cano}}, \end{aligned} \tag{26}$$

$$\left(c_e^{\mathrm{sGC}} - c_c^{\mathrm{sGC}}\right) - \left(c_e^{\mathrm{Cano}} - c_c^{\mathrm{Cano}}\right) = -\frac{c\,(1-c)}{n}\frac{e^{\underline{\tau}}\,(e^{\underline{\tau}}-1)}{(1-c+ce^{\underline{\tau}})^3}. \tag{27}$$

Whatever the chain length, $c_e^{\mathrm{sGC}} < c_e^{\mathrm{Cano}}$ [Fig. 5(a)], which is in a good agreement with Eq. (26) since $\underline{\tau} > 0\,(e^{\underline{\tau}} - 1 > 0)$. Figure 5(b) also indicates that for core sites, $c_c^{\mathrm{sGC}} > c_c^{\mathrm{Cano}}$, contrary to what Eq. (26) predicts. This comes from the fact that the edge and core site concentrations are related via the mass conservation law Eq. (5) so that we have $c_c^{\mathrm{sGC}} - c_c^{\mathrm{Cano}} = \frac{-2}{n-2}(c_e^{\mathrm{sGC}} - c_e^{\mathrm{Cano}})$. The difference in core concentration is an order smaller (in $1/n$) than the difference in edge concentration. A second order expansion must be taken to see the difference in concentration.

It is straightforward to relate it to the Delta method formalism, which yields:

$$c_p^{\mathrm{sGC}} - c_p^{\mathrm{Cano}} = \frac{\sigma^2}{2}\frac{\partial^2 c_p^{\mathrm{Cano}}}{\partial c^2}, \tag{28}$$

by noticing that the first-order term in $1/n$ is

$$\sigma^2 = c\,(1-c)\,/n, \tag{29}$$

and

$$\begin{aligned} \frac{\partial^2 c_e^{\mathrm{Cano}}}{\partial c^2} &= -\frac{2e^{\underline{\tau}}\,(e^{\underline{\tau}}-1)}{(1-c+ce^{\underline{\tau}})^3}, \\ \frac{\partial^2 c_c^{\mathrm{Cano}}}{\partial c^2} &= \frac{4}{n}\frac{e^{\underline{\tau}}\,(e^{\underline{\tau}}-1)}{(1-c+ce^{\underline{\tau}})^3}. \end{aligned} \tag{30}$$

The deviation observed between both ensembles for c_c [Figs. 4(e) and 5(b)] is of lower order than that obtained for c_e and requires one to account for the first-order term in the curvature of $c_c^{\mathrm{Cano}}(c)$ (i.e., a second-order term for $c_c^{\mathrm{sGC}} - c_c^{\mathrm{Cano}}$).

Equation (29) provides a very good approximation of σ^2, represented in Fig. 7(a) for $n = 30$ and $n = 5$, as a decreasing function of n, whatever the nominal concentration, as expected. Figure 7(b) shows that the curvature of the edge concentrations depends on the chain length for low concentrations, contrary to what the simplified formula in Eq. (30) predicted for larger chains. Nevertheless the simplified formula of Eq. (28) is in satisfying agreement with both exact computations and the Delta method formula without approximation. Thus, the length dependence of the deviation

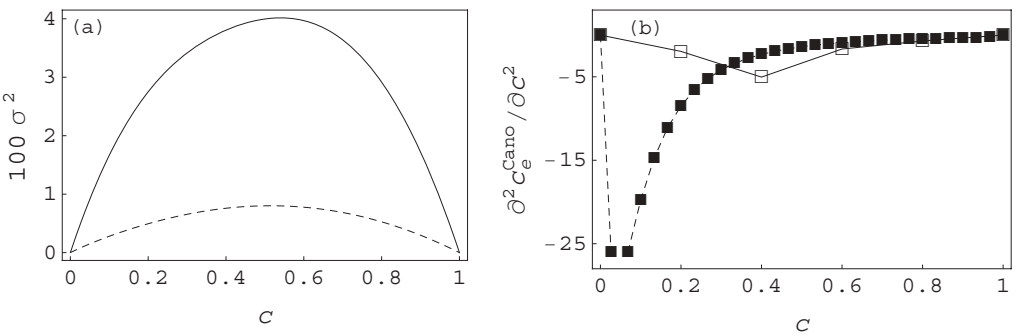

FIG. 7. Evolution (a) of the nominal concentration variance in the sGC ensemble and (b) of the canonical edge isotherm curvature as a function of the nominal concentration for $n = 10$ (lines and open squares) and $n = 30$(dashed lines and filled squares) at $\underline{\tau} = 2$.

between both ensembles is mainly due to variance. For core sites, accounting for the first-order term in the curvature of Eq. (30) describes the curvature of small chains correctly and achieves a good approximation of $c_c^{\mathrm{sGC}} - c_c^{\mathrm{Cano}}$.

Note that approximate expressions of isotherms $c(\underline{\Delta\mu})$

$$\underline{\Delta\mu}^{\mathrm{Cano}} = 2\underline{\tau} + \ln\frac{c}{1-c} + \frac{1}{2n}\frac{1-2c}{c\,(1-c)} - \frac{2}{n}\frac{e^{\underline{\tau}}-1}{1-c+ce^{\underline{\tau}}} \tag{31}$$

and

$$c^{\mathrm{sGC}} = \frac{1}{1+e^{2\underline{\tau}-\underline{\Delta\mu}}}\left[1+\frac{2}{n}\frac{(e^{\underline{\tau}}-1)\times e^{\underline{\tau}-\underline{\Delta\mu}}}{1+e^{\underline{\tau}-\underline{\Delta\mu}}}\right] \tag{32}$$

are also in a good agreement with exact computations.

B. Influence of temperature

To illustrate the influence of temperature, T, we present isotherms $c(\underline{\Delta\mu})$ obtained for $\underline{\tau}=4$ [Fig. 8(a)] and $\underline{\tau}=8$ [Fig. 8(b)] for $n=10$. This means that the initial temperature (for $\underline{\tau}=2$) is divided by two and four, respectively. The larger $\underline{\tau}$ is, the more the isotherms are shifted toward higher values of $\underline{\Delta\mu}$. At very low temperatures ($\underline{\tau}=8$), the isotherm shows a plateau for $c\approx 0.2 = 2/n$ [Fig. 8(b)]. The lower the temperature, the more disconnected the core and edge site enrichments [Figs. 8(c) and 8(d)]. For very low temperatures ($\underline{\tau}=8$), Fig. 8(d) shows two distinct domains:

(1) For $c<2/n$, the edge concentration goes up to 1, whereas the core concentration remains nil; thus, at $c\approx 2/n$, only the edge sites are enriched by A atoms. Core sites being pure in B atoms, the nanowire then presents a core shell structure.

(2) For $c>2/n$, the core concentration increases linearly with c.

This complete decoupling of the isotherms of the different sites has a strong effect on the shape of the curve $\sigma^2(c)$. Compared with $\underline{\tau}=2$, the evolution of variance with concentration for $\underline{\tau}=4$, shown in Fig. 9(a), is less symmetrical, and σ^2 is slightly lower for intermediate concentrations. At $\underline{\tau}=8$, two distinct domains of the curve $\sigma^2(c)$ [Fig. 9(b)] appear. The variance being proportional with $\partial c/\partial\underline{\Delta\mu}$, the extremum of $\sigma^2(c)$ corresponds to the extremum of the slope of the isotherm $c(\underline{\Delta\mu})$ [Figs. 8(a) and 8(b)]. So, the maximum of the first domain, which corresponds to the increase in edge concentration, occurs at $c_e\approx 1/2$ ($c\approx 1/n$). When the isotherm presents a plateau [Fig. 8(b)], $c\approx 2/n$, with $c_e\approx 1$ and $c_c\approx 0$, and σ^2 is close to 0 [Fig. 9(b)]. The second maximum occurs at $c_c\approx 1/2$ ($c_e\approx 1$).

At low temperature, the curvature of the canonical isotherm is close to zero, except for concentrations around $c\approx 2/n$ [Figs. 9(c) and 9(d)]. As before, the deviation between the approximate and the exact concentration profiles is very weak, even for $c\approx 2/n$, as shown in Figs. 9(e) and 9(f).

Figure 10 shows that the temperature evolution of the deviation between both ensembles depends on the concentration to be investigated.

The concentration range in which this deviation is not nil diminishes when temperature diminishes. The maximal deviation is obtained for $c=2/n$ and has a relatively complex temperature dependency, as analyzed in Table I. The decrease in temperature (i.e., the increase of $\underline{\tau}$) leads to two opposite effects: the decrease of the concentration fluctuations around its average value in the sGC ensemble and the increase of the absolute value of the curvature of the canonical isotherms.

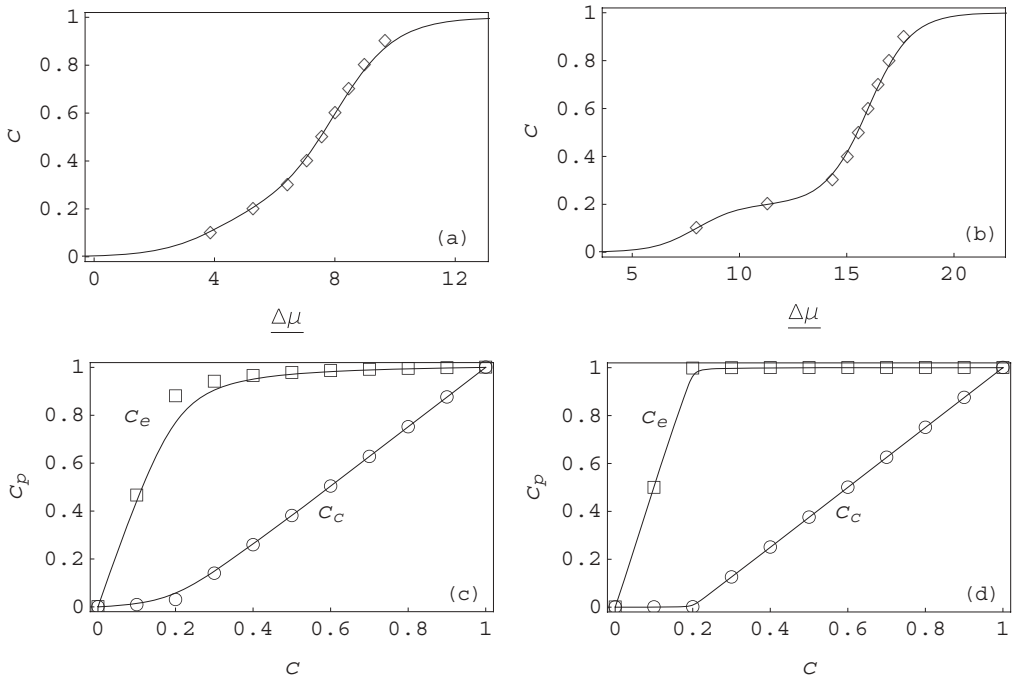

FIG. 8. Nominal concentration isotherm as a function of the chemical potential difference $\underline{\Delta\mu}$ for $\underline{\tau}=4$ (a) and $\underline{\tau}=8$ (b) in both ensembles (sGC, line; canonical, diamond). Edge and core concentration isotherms as a function of the nominal concentration for $\underline{\tau}=4$ (c) and $\underline{\tau}=8$ (d) in the sGC ensemble (line) and the canonical ensemble (squares for the edge sites and circles for the core sites). $n=10$.

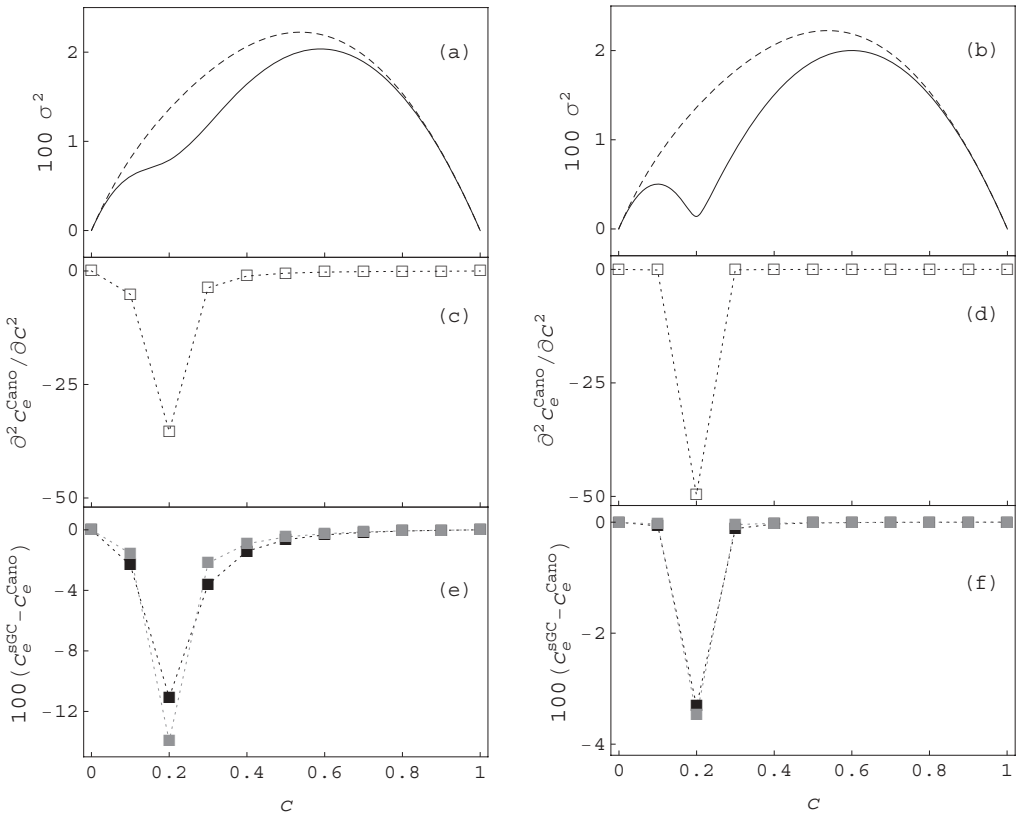

FIG. 9. Evolution with nominal concentration of (a, b) the variance, (c, d) the canonical edge isotherm curvature, and (e, f) the difference between the sGC and canonical edge concentrations for $\underline{\tau} = 4$ (a, c, e) and $\underline{\tau} = 8$ (b, d, f). $\sigma^2(c)$ for $\underline{\tau} = 2$ is noted with a dashed line in panels a and b. Dotted lines are visual aids in panels c–f. Solid black symbols denote exact solid gray symbols denote approached results given by Eq. (21) in panels e and f. $n = 10$.

Table I indicates that this can lead to a nonmonotonic variation of $c_e^{\mathrm{sGC}} - c_e^{\mathrm{Cano}}$ with the temperature.

V. CONCLUSIONS

We have shown that even for an A_cB_{1c} alloy forming an ideal solid solution, different statistical ensembles are not equivalent for small systems as the mixing entropy overestimates the configurational entropy in the canonical ensemble. Consequently, the average of a thermodynamic variable taken in a canonical ensemble is not equal to the average taken in the sGC ensemble. Thus, to compare theoretical and experimental results, the choice of the pertinent statistical ensemble is crucial. A canonical ensemble should be employed to calculate the properties of a chemically isolated cluster, whereas for an alloyed cluster in equilibrium with a reservoir, or for a collection of clusters in mutual equilibrium, the sGC ensemble should be used.

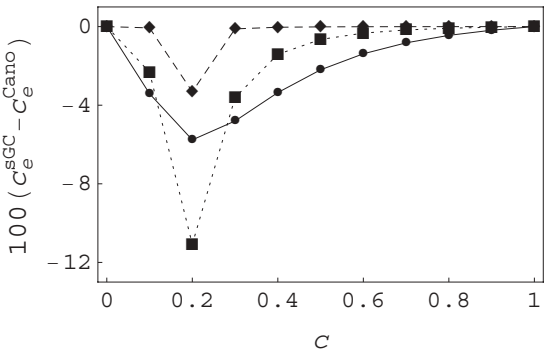

FIG. 10. Difference between the sGC and canonical edge concentrations as a function of the nominal concentration for $\underline{\tau} = 2$ (point), $\underline{\tau} = 4$ (square), and $\underline{\tau} = 8$ (diamond). Lines are visual aids. $n = 10$.

The Delta relationship enables us to link both ensembles and to analyze their difference. We have shown that the canonical isotherms $c(\underline{\Delta\mu})$ and $c_p(\underline{\Delta\mu})$ are steeper than the sGC isotherms. The deviation between both ensembles is proportional, on the one hand, to the amplitude of the fluctuations of the nominal concentration in the sGC ensemble and, on the other hand, to the curvature of the canonical isotherm considered at the given nominal concentration. This study emphasizes that the deviation between both ensembles:

TABLE I. Evolution of the variance, absolute value of the curvature of the canonical edge isotherm, and value of $c_e^{\mathrm{sGC}} - c_e^{\mathrm{Cano}}$ with $\underline{\tau}$ at $c = 2/n$ for $n = 10$.

$\underline{\tau}$	$100\sigma^2$	$\lvert\partial^2 c_e^{\mathrm{Cano}}/\partial c^2\rvert$	$100(c_e^{\mathrm{sGC}} - c_e^{\mathrm{Cano}})$
2	1.4	10	−5.7
4	0.8	35	−11
8	0.14	50	−3.3

(1) decreases with an increase in chain length, mainly because of the decrease in fluctuations for a given value of the nominal concentration, and

(2) presents various behaviors in temperature for a given chain length, depending on the value of the nominal concentration to be considered. On one hand, the concentration range for which there exists a discrepancy between both ensembles increases with temperature. On the other hand, the maximum of the deviation does not vary monotonically with temperature.

We have shown that segregation at the edge sites, characterized by $c_e - c_c$, is greater in the canonical ensemble than in the sGC ensemble, whatever the nominal concentration. The segregation increases (resp. decreases) with the length of the chain for low (resp. high) nominal concentration in both ensembles. In an intermediate range of concentrations, segregation decreases with length in the canonical ensemble, whereas it increases in the sGC ensemble.

The connection between the canonical ensemble and the sGC ensemble remains to be specified for alloys with a tendency to phase separate. In that case, we previously showed that the configurational state density displays two modes at low temperature.[21] Concentration profiles and isotherms then differ strongly between both ensembles. One can wonder whether the Delta formalism is still valid and efficient for investigating differences between both ensembles. This study will be extended to the study of submonolayer 1D codeposition and to modeling of the kinetics of codeposition using cluster dynamics. Finally, we hope this may help and stimulate an experimental analysis of composition profiles within bimetallic particles.

ACKNOWLEDGMENTS

The authors thank M. Briki, F. Lequien, and J. Creuze for very fruitful discussions.

APPENDIX A

In this Appendix, we express the exact sGC concentration profiles as a function of the nominal concentration. With regard to Eq. (10), one can write c_c^{sGC} directly as a function of c_e^{sGC}:

$$c_c^{\mathrm{sGC}} = \frac{c_e^{\mathrm{sGC}}}{c_e^{\mathrm{sGC}} + e^{\underline{\tau}}(1 - c_e^{\mathrm{sGC}})}. \tag{A1}$$

The mass conservation law Eq. (5) then becomes

$$2(1 - e^{\underline{\tau}})\left(c_e^{\mathrm{sGC}}\right)^2 + [(n-2) - nc^{\mathrm{sGC}}(1 - e^{\underline{\tau}}) + 2e^{\underline{\tau}}]c_e^{\mathrm{sGC}} - nc^{\mathrm{sGC}}e^{\underline{\tau}} = 0. \tag{A2}$$

Thus, we obtain the following relations:

$$\begin{aligned} c_e^{\mathrm{sGC}} &= \frac{-(n-2) + nc^{\mathrm{sGC}}(1 - e^{\underline{\tau}}) - 2e^{\underline{\tau}} - \sqrt{8e^{\underline{\tau}}(n-2) + [-(n-2) + nc^{\mathrm{sGC}}(1 - e^{\underline{\tau}}) + 2e^{\underline{\tau}}]^2}}{4(1 - e^{\underline{\tau}})}, \\ c_c^{\mathrm{sGC}} &= \frac{(n-2) + nc^{\mathrm{sGC}}(1 - e^{\underline{\tau}}) + 2e^{\underline{\tau}} - \sqrt{8e^{\underline{\tau}}(n-2) + [-(n-2) + nc^{\mathrm{sGC}}(1 - e^{\underline{\tau}}) + 2e^{\underline{\tau}}]^2}}{2(1 - e^{\underline{\tau}})(n-2)}. \end{aligned} \tag{A3}$$

APPENDIX B

The exact canonical concentration profiles can be obtained from the canonical partition function

$$Z^{\mathrm{Cano}} = \sum_{n_{\mathrm{A},e}=0}^{2} Z_{n_{\mathrm{A},e}}^{\mathrm{Cano}} \text{ with } Z_{n_{\mathrm{A},e}}^{\mathrm{Cano}} = N_{n_{\mathrm{A},e}}^{\mathrm{Cano}} \exp[-\underline{H}(n, n_{\mathrm{A}}, n_{\mathrm{A},e})], \tag{B1}$$

where $N_{n_{\mathrm{A},e}}^{\mathrm{Cano}}$ represents the number of configurations when $n_{\mathrm{A},e}$ atoms are situated on edge sites.

$$Z_{p_i=1}^{\mathrm{Cano}} = \sum_{n_{\mathrm{A},e}=0}^{2} Z_{p_i=1,n_{\mathrm{A},e}}^{\mathrm{Cano}}, \; Z_{p_i=1,n_{\mathrm{A},e}}^{\mathrm{Cano}} = N_{p_i=1,n_{\mathrm{A},e}}^{\mathrm{Cano}} \exp[-\underline{H}(n, n_{\mathrm{A}}, n_{\mathrm{A},e})], \tag{B2}$$

$$N_{n_{\mathrm{A},e}}^{\mathrm{Cano}} = \binom{2}{n_{\mathrm{A},e}} \binom{n-2}{n_{\mathrm{A}} - n_{\mathrm{A},e}},$$

and

$$N_{p_i=1,n_{\mathrm{A},e}}^{\mathrm{Cano}} = \binom{z_i}{n_{\mathrm{A},e} - 2 + z_i} \binom{n - 1 - z_i}{n_{\mathrm{A}} + 1 - z_i - n_{\mathrm{A},e}}. \tag{B3}$$

*emile.maras@u-psud.fr

[1] J. H. Sinfelt, *Bimetallic Catalysts: Discoveries, Concepts and Applications* (Wiley, New York, 1983).

[2] R. Ferrando, J. Jellinek, and R. L. Johnston, Chem. Rev. **108**, 845 (2008).

[3] H. Zeng, J. Li, Z. L. Wang, J. P. Liu, and S. Sun, Nano Lett. **4**, 187 (2004).

[4] M. Gaudry, E. Cottancin, M. Pellarin, J. Lermé, L. Arnaud, J. R. Huntzinger, J. L. Vialle, M. Broyer, J. L. Rousset, M. Treilleux, and P. Mélinon, Phys. Rev. B **67**, 155409 (2003).

[5]J. Gonzalo, D. Babonneau, C. N. Afonso, and J. P. Barnes, J. Appl. Phys. **96**, 5163 (2004).
[6]G. Timp, R. E. Howard, and P. Mankiewich, in *Nanotechnology*, edited by G. Timp (Springer-Verlag, New York, 1999), pp. 8–87.
[7]M. Wautelet, Phys. Lett. A **246**, 341 (1998).
[8]V. Damora Das and D. Karunakaran, J. Appl. Phys. **68**, 2105 (1990).
[9]F. Ducastelle, *Order and Phase Stability in Alloys* (North-Holland, Amsterdam, 1991).
[10]G. Tréglia, B. Legrand, F. Ducastelle, A. Saul, C. Gallis, I. Meunier, C. Mottet, and A. Senhaji, Comput. Mater. Sci. **15**, 196 (1999).
[11]F. Lequien, J. Creuze, F. Berthier, I. Braems, and B. Legrand, Phys. Rev. B **78**, 075414 (2008).
[12]M. Polak and L. Rubinovich, Phys. Rev. B **71**, 125426 (2005).
[13]G. Wang, M. A. Van Hove, P. N. Ross, and M. I. Baskes, J. Chem. Phys. **122**, 024706 (2005).
[14]G. Lehaut, F. Gulminelli, and O. Lopez, Phys. Rev. E **81**, 051104 (2010).
[15]L. Van Hove, Physica **15**, 951 (1949).
[16]F. Gulminelli, Ann. Phys. Fr. **29**, 1 (2004).
[17]P. Chomaz, V. Duflot, and F. Gulminelli, Phys. Rev. Lett. **85**, 3587 (2000).
[18]J. Creuze, F. Berthier, and B. Legrand, in *Nanoalloys: Synthesis, Structure and Properties*, edited by Damien Alloyeau, Christine Mottet, and Christian Ricolleau (Springer Verlag, London, 2012), Chap. 7, pp. 227–257.
[19]F. Lequien, J. Creuze, F. Berthier, and B. Legrand, Faraday Discuss. **138**, 105 (2008).
[20]M. Briki, J. Creuze, F. Berthier, and B. Legrand, Solid State Phenom. **172–174**, 658 (2011).
[21]F. Lequien, Ph.D. thesis, Univ. Paris Sud, Orsay, France, 2008.
[22]J. Creuze, I. Braems, F. Berthier, C. Mottet, G. Treglia, and B. Legrand, Phys. Rev. B **78**, 075413 (2008).
[23]E. Maras, I. Braems, and F. Berthier, Sol. State Phenom. **172–174**, 676 (2011).
[24]M. B. Yilmaz and F. M. Zimmermann, Phys. Rev. E **71**, 026127 (2005).
[25]S. I. Denisov and P. Hänggi, Phys. Rev. E **71**, 046137 (2005).
[26]F. Berthier, E. Maras, I. Braems, and B. Legrand, Acta Mat. **58**, 2387 (2010).
[27]P. Gambardella, H. Brune, K. Kern, and V. I. Marchenko, Phys. Rev. B **73**, 245425 (2006).
[28]P. Gambardella, M. Blanc, K. Kuhnke, K. Kern, F. Picaud, C. Ramseyer, C. Girardet, C. Barreteau, D. Spanjaard, and M. C. Desjonqueres, Phys. Rev. B **64**, 045404 (2001).
[29]B. Diu, C. Guthmann, D. Ledere, and B. Roulet, *Physique Statistique* (Hermann, Paris, 1989).
[30]C. Bichara, J.-P. Gaspard, and J.-C. Mathieu, J. Chem. Phys. **89**, 4339 (1988).
[31]I. Braems and F. Berthier, Sol. State Phenom. **172–174**, 1038 (2011).
[32]Bernard Picinbono, *Signaux aléatoires: avec problèmes résolus* (Dunod, Paris, 1995).
[33]W. Feller, *An Introduction to Probability Theory and Its Applications* (Wiley, New York, 1968), Vol. 1, Sec. VII.3.
[34]G. W. Oehlert, The American Statistician **46**, 27 (1992).